Total energy loss to fast ablator-ions and target capacitance of direct-drive implosions on OMEGA

N. Sinenian, A. B. Zylstra, M. J.-E. Manuel, H. G. Rinderknecht, J. A. Frenje et al.

Citation: Appl. Phys. Lett. **101**, 114102 (2012); doi: 10.1063/1.4752012
View online: http://dx.doi.org/10.1063/1.4752012
View Table of Contents: http://apl.aip.org/resource/1/APPLAB/v101/i11
Published by the American Institute of Physics.

Total energy loss to fast ablator-ions and target capacitance of direct-drive implosions on OMEGA

N. Sinenian,[1,a)] A. B. Zylstra,[1] M. J.-E. Manuel,[1] H. G. Rinderknecht,[1] J. A. Frenje,[1] F. H. Séguin,[1] C. K. Li,[1] R. D. Petrasso,[1] V. Goncharov,[2] J. Delettrez,[2] I. V. Igumenshchev,[2] D. H. Froula,[2] C. Stoeckl,[2] T. C. Sangster,[2] D. D. Meyerhofer,[2] J. A. Cobble,[3] and D. G. Hicks[4]

[1]*Plasma Science and Fusion Center, Massachusetts Institute of Technology, Cambridge, Massachusetts 02139, USA*
[2]*Laboratory for Laser Energetics, Rochester, New York 14623, USA*
[3]*Los Alamos National Laboratory, Los Alamos, New Mexico 87545, USA*
[4]*Lawrence Livermore National Laboratory, Livermore, California 94550, USA*

(Received 31 July 2012; accepted 28 August 2012; published online 10 September 2012)

Measurements of the total energy carried by fast ablator-ions in direct-drive implosions on OMEGA have been conducted using magnetic and Thomson Parabola spectrometers. It is shown that the total laser energy lost to fast ablator-ions for plastic and glass targets is comparable and that it is a modest fraction of the incident laser energy ($\lesssim$1%). These measurements have been used to infer a non-linear, voltage-dependent target capacitance ($\sim$0.1 nF) associated with the space-charge that accelerates the fast-ions. © *2012 American Institute of Physics*. [http://dx.doi.org/10.1063/1.4752012]

Energetic fast protons ($\gtrsim$1 MeV) and electrostatic charging of targets have been previously observed in direct-drive[1] and indirect-drive[2] inertial confinement fusion (ICF) implosions on the OMEGA laser.[3] These fast protons, sourced from water-vapor and other surface contaminants, have total yields of $\sim 10^{13}-10^{14}$ and are accelerated by hot-electrons that are generated by laser-plasma interactions (LPI). It has been shown previously for surrogate plastic and glass targets that the maximum proton energies measured on OMEGA, corresponding to the peak target voltage, scale with the on-target laser intensity as $\sim I\lambda^2$. This is stronger than the $(I\lambda^2)^{1/3}$ scaling associated with resonance absorption (RA) that is widely observed in other experiments.[4,5] In addition, it has been shown that these protons carry less than 0.3% of the laser energy.[1] Finally, the late-time behavior of the target voltage has been inferred[6] and associated return currents have been studied.[7–9]

In this letter, we address two significant outstanding questions: (1) the total amount of laser energy coupled to *all* fast ions and (2) the capacitance associated with the charge-separation surrounding the target. The former was obtained through measurements of heavy fast ions from several different target (ablator) materials. The latter was derived by interpreting these measurements as a non-linear target capacitance associated with the sheath fields surrounding the target.

The total amount of laser energy coupled to fast-ablator ions is important for studies of preheat in ICF implosions. A fraction of the incident laser energy is coupled to hot-electrons ($T_{hot} \sim 10-100$ keV) by the two-plasmon decay (TPD) instability.[10] The fastest of these electrons escape the target and leave behind a positive potential that accelerates ablator-ions from the coronal plasma. The remaining electrons become trapped within this potential well and can deposit their energy into the fuel, increasing the fuel adiabat and degrading the target compression. The amount of incident laser energy coupled to hot-electrons is a topic of current investigation, but recent estimates in a planar geometry relevant to direct-drive implosions suggest that less than 1% of the incident laser energy is coupled to hot-electrons.[11] This amount ($\sim$200 J) is substantial in the context of hot-electron preheat of the target. It has been estimated that preheat of cryogenic targets at OMEGA in the amount of $\sim$10 J can degrade target compression and reduce the areal density (ρR) by 20%.[12] If the fraction of hot-electron energy coupled to fast-ions is known, an upper bound is obtained on the electron energy available for preheat.

Equally important for preheat studies is the time-constant over which the target potential is present, trapping electrons and allowing deposition of hot-electron energy into the fuel. The time-constant for the voltage decay is partly determined by the target capacitance.[13] For a given peak target voltage, the capacitance determines the total amount of energy coupled to fast ablator ions and can be inferred from the measurements presented here.

Measurements were conducted at the OMEGA laser facility[3] (30 kJ, 60-beam, $\lambda_L = 0.33\ \mu$m) for a variety of target parameters. The spherical targets, with diameters ranging from $400-860\ \mu$m, were composed of either plastic (CD or CH) or glass (SiO_2) with wall thicknesses ranging from $2-27\ \mu$m. These targets were filled with either DT, D_2, or D^3He gas. In some cases, the targets were flash-coated with 100 nm of aluminum to mitigate diffusion of ^{3}He. Cryogenic targets, with a plastic (CD) shell and an inner layer of DT or D_2 ice ($\sim 100\ \mu$m), were also studied.[12] The on-target laser energy ($\sim$20 kJ) and pulse duration ($\sim 1-3$ ns) were varied to achieve on-target intensities in the range of $10^{14}-10^{15}$ W-cm^{-2}. The laser pulse shapes used in this study were square or shaped and in some cases preceded by either a single or triple picket.

Fast ablator proton and deuteron energy spectra were measured using the magnet-based charged-particle

a)Electronic mail: nareg@psfc.mit.edu.

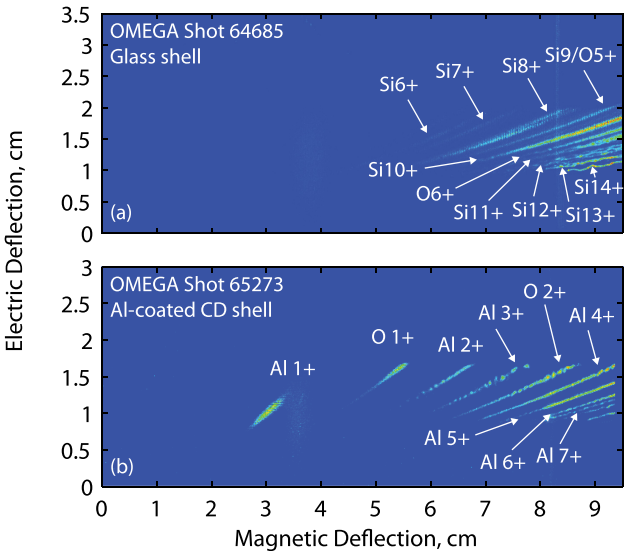

FIG. 1. Data recorded by a CR-39 detector in the TP spectrometer is for a glass-shell (a) and an aluminum flash-CD shell (b). Each pixel represents a number of heavy-ion particle tracks. The local track density was then mapped to a color value to produce these "images." Several lines of highly ionized silicon and oxygen (from glass shells) and aluminum and oxygen (from flash-coated CD shells) were measured. The TP was run with peak magnetic and electric fields of 5.4 kG and 2.8 kV-cm^{-1}, respectively.

spectrometers (CPS1 and CPS2).[14] A Thomson Parabola (TP)[15] with parallel electric and magnetic fields was used for spectral measurements of heavier fast ablator-ions (C, Si, O, Al). These instruments use CR-39 solid-state nuclear track detectors (SSNTD),[14,16] and are immune to EMP and x-rays.

Data recorded by CR-39 detectors in the TP are shown in Fig. 1. Glass and plastic (CD) targets show several strong lines of heavy ions, including silicon, oxygen, and aluminum. In some cases several weaker lines, not visible in these images, including charge states of carbon were detected and recorded. It was found that the majority of energy is carried by highly ionized charge states of silicon (for glass) and aluminum (for flash-coated CD targets). Sample energy spectra of these fast heavy-ions are shown in Fig. 2 alongside proton spectra acquired using CPS1.

For each shot, spectra similar to those shown in Fig. 2 were integrated to obtain the total energy carried by fast ablator-ions. Fig. 3 shows the percentage of laser energy carried by fast ablator-ions as a function of the peak voltage on the target, which was determined by measuring the energy of

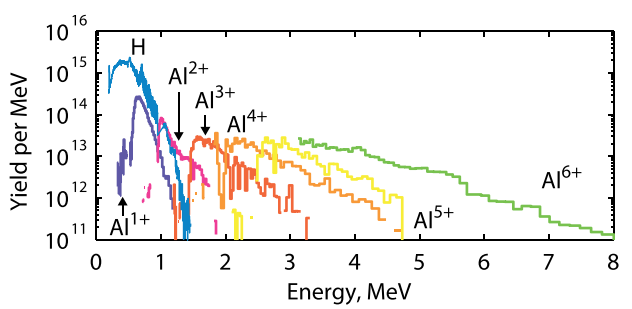

FIG. 2. Energy spectra of fast ablator-ions, including several charge-states of aluminum alongside protons from a flash-coated CD target (OMEGA Shot 65273). For this shot, the maximum proton energy, corresponding to the peak target voltage, was 1.35 MeV.

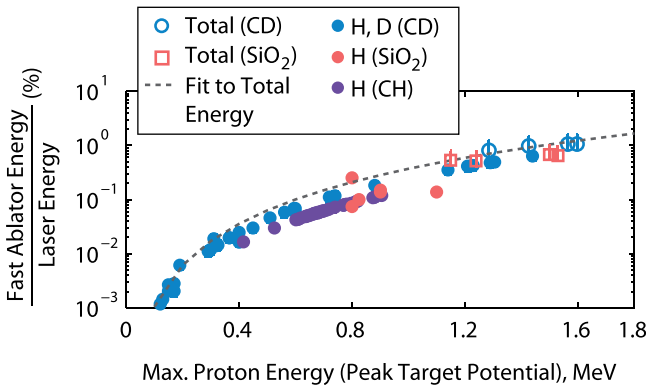

FIG. 3. Percentage of incident laser energy carried by fast ablator-ions, including protons from CH and SiO_2 shells ($\lesssim 0.3\%$), protons and deuterons from CD shells ($\lesssim 0.6\%$), and heavier fast ions CD and SiO_2 ($\lesssim 0.3\%$). The total incident laser energy coupled to fast ablator-ions (dashed curve) is estimated by scaling the CD dataset (solid blue circles) to match the total ion measurements (open blue circles). Where not shown, the error-bars are comparable to the symbol size.

the fastest ablator-proton. These data incorporate protons from CH and glass targets, protons and deuterons from CD targets (solid symbols) and the total energy carried by all ion species for a few CD and glass targets (open symbols). The latter data show that the total energy carried by fast ablator-ions is comparable between CD and glass targets for a given potential. Neither laser pulse parameters nor target metrology affect the shape or the magnitude of the curves shown here, as each of them incorporate a variety of target parameters (diameters and thicknesses) and laser parameters (laser energies, pulse duration and pulse shapes). This demonstrates that the fraction of laser energy carried by fast ablator-ions is a unique function of the peak target potential.

Based on the measurement of the total energy carried by fast ablators in glass and CD targets for voltages between 1–1.5 MeV, we estimate that heavy fast-ions carry nearly as much energy as their proton and deuteron counterparts. The comprehensive dataset for CD is described by a power law dependence on the target voltage (reduced $\chi^2 = 0.99$), and then scaled to match the total energy loss measurement for CD shells, resulting in the dashed curve shown in Fig. 3. From the fit, the fraction of incident laser energy carried by fast ablator-ions is given by

$$f_E = 3.7 \times 10^{-3} V_{0,MV}^{2.55}, \quad (1)$$

where $V_{0,MV}$ is the maximum proton energy (in megavolts) that corresponds to the peak target voltage for each shot. The upper error bars of the total ion energy measurement and hence the uncertainty in the above fit are determined by the accuracy of the measurement. The low-energy cutoff of the TP (1.6 MeV proton equivalent) precludes measurement of the spectrum at lower energies, resulting in an underestimate of the total energy by no more than 40–50%. This effect varies from one ion-species to the next and depends on the spectral shape, but for most ions shown here, the majority of the spectrum is measured. The lower error-bars for the total ion energy measurement are a result of instrument precision (25%) that is determined by uncertainties in the energy calibration of the TP. The magnetic spectrometers CPS1 and CPS2 measure proton and deuteron spectra down to

100 keV, resulting in precision-dominated error bars (±25%) for the measurements of the energy carried by the light ions shown in Fig. 3.

The capacitance across the sheath surrounding the target can be inferred from Eq. (1). The dashed curve in Fig. 3 can be thought of as the energy stored in a capacitor ($E_T = 1/2CV_0^2$) that is initially charged to a peak voltage (V_0). Since the power-law fit of Eq. (1) is normalized to laser energy and has an exponent >2, we expect the capacitance to scale with laser energy and exhibit a power-law dependence on the voltage. Taking $C \sim \beta E_L V^{\alpha}$, where α and β are constants to be determined from the data, the total energy stored in the capacitor is given by

$$E_T = \int_0^{V_0} \beta E_L V^{1+\alpha} dV = \beta E_L V_0^{2+\alpha}/(2+\alpha). \quad (2)$$

Comparing this equation with Eq. (1), the target capacitance is inferred to be

$$C_T = 9.4 E_L V_{MV}^{0.55}\ \text{pF}, \quad (3)$$

where V_{MV} is the instantaneous target voltage (in megavolts) and E_L is the incident laser energy (in kilojoules). This scaling is valid for laser energies in the range of 20–30 kJ and target voltages of 0.1–1.6 MV. The target capacitance is an implicit function of time since the target voltage evolves over the laser pulse duration.[6] For peak target voltages of 0.1–1 MV and an incident laser energy of 20 kJ, the initial capacitance is approximately 50–190 pF. This result can be compared to the capacitance of two concentric spheres in vacuum, given by $4\pi\epsilon_0/(r_i^{-1} - r_o^{-1})$. Taking the inner radius to be that of the target ($r_t \approx 0.5$ mm) and outer radius to be the sum of the target radius and the initial hot-electron Debye length ($\lambda_D \sim 0.1$–$0.2\,\mu$m for $T_{hot} \sim 50-100$ keV) gives a capacitance of 140–280 pF, which is of the same order as the inferred capacitance.

Since the energy loss to fast ablator-ions is parameterized by the peak voltage, it is important to examine what parameters dictate the initial voltage on target. A previous study showed that the target voltage scales with the on-target intensity[1] and that it was larger for thin <5 μm CH shells in comparison to thick >5 μm shells. We extend that study to include data from cryogenic and warm CD-shells (see Fig. 4) with a variety of shell thicknesses (3–10 μm-thick) in addition to CH-shells (15–27 μm-thick) and thin glass shells (2–3 μm).

Thin glass shells follow the scaling of thicker shells, resulting in lower peak target voltages for a given intensity than thin plastic shells. The observed discrepancy between thin glass and thin plastic shells is due to differences in shell absorption of laser light and hot-electron stopping power. Higher collisional absorption of incident laser light for higher-Z thin glass shells relative to thin plastic shells leads to higher coronal temperatures (T_c) and lower laser intensities at the quarter-critical surface. These conditions can mitigate the TPD instability, which has a threshold parameter $\eta \propto I/T_c$.[17] In addition, the path-integrated hot-electron stopping power ($\Delta E = \int dE/ds\, ds$) of thin glass shells is greater than that of thin plastic shells (for 50–100 keV electrons, $\Delta E_{SiO2}/\Delta E_{CD,Thin} \approx 2$–4). Thus, any hot-electrons that are produced are more readily stopped by thin glass shells,

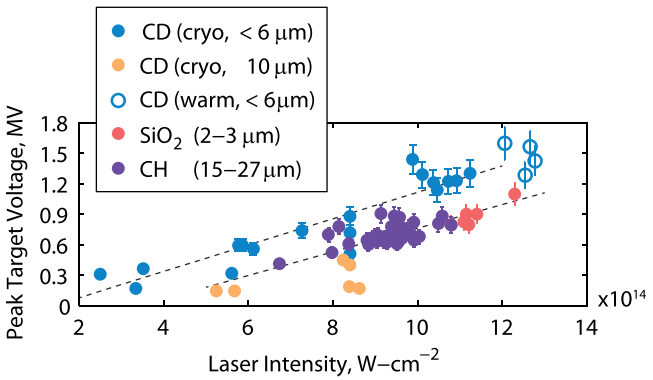

FIG. 4. Peak target voltage as a function of the on-target laser intensity. Cryogenic and warm thin plastic shells (<6 μm) exhibit a linear dependence with laser intensity. Thick plastic shells (>10 μm) and thin glass shells (2−3 μm) also follow a linear scaling with intensity, but result in peak voltages that are systematically lower. These discrepancies are due to differences in shell laser absorption and electron stopping power.

resulting in lower peak target voltages. For thin glass and thick plastic shells, the scaling with intensity is given by (reduced $\chi^2 = 0.78$)

$$V_{0,MV} = 0.12 I_{14} - 0.4, \quad (4)$$

where $V_{0,MV}$ is the peak target voltage in megavolts and I_{14} is the laser intensity in units of 10^{14} W-cm^{-2}. For thin plastic shells, the peak voltage is systematically higher (reduced $\chi^2 = 0.89$)

$$V_{0,MV} = 0.13 I_{14} - 0.18. \quad (5)$$

Shell absorption arguments can also explain the difference between thin and thick plastic shells. It has been shown for cryogenic targets that thicker shells prevent the laser from burning through to the lower-Z D_2 or DT ice-layer.[12] For thinner shells that burn through, it has been suggested that the lower-Z deuterium plasma penetrates into the underdense region, resulting in lower collisional absorption of laser light. This creates conditions that are favorable for the TPD instability and hence the generation of hot-electrons.[12]

For these data, distributed phase plates (DPP)[18] and distributed polarization rotators (DPR)[19] were used to shape the spatial profile of the laser beam and to randomize the laser polarization, respectively. On some shots, laser speckles were smoothed using Smoothing by Spectral Dispersion (SSD).[20] The observed scatter in the cryogenic data is attributed to the wide range of pulse shapes used in these experiments. Scatter in warm-plastic and glass targets is largely due to uncertainties in the measurement of the peak target potential. For these shells, pulse shapes (1 ns, square) and SSD modulations were comparable.

The observed linear scaling of the maximum fast ablator-proton energy with laser intensity (as opposed to the commonly observed $\propto (I\lambda^2)^{1/3}$ scaling[4,5] associated with RA) is explained by the fact that these protons are accelerated by TPD-generated hot-electrons. It has been shown that the temperature of these electrons scales linearly with laser intensity,[11,21] and there is a linear relationship between the maximum fast-proton energy and the hot-electron temperature.[22]

Previous experiments[23,24] confirmed that the dominant mechanism for hot-electron production for OMEGA

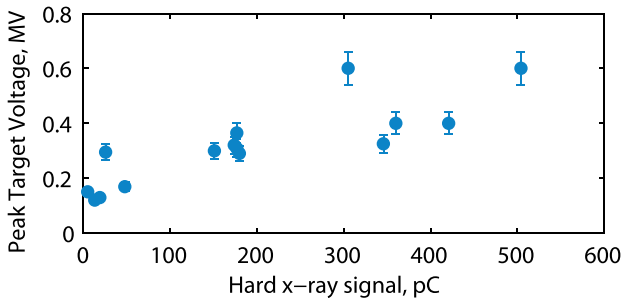

FIG. 5. Target voltage for D_2 cryogenic implosions as a function of the hard x-ray signal (shown here as the charge collected on the hard x-ray detector). The hard x-rays are from bremsstrahlung radiation (photon energies >40 keV) produced by hot-electrons stopping on the shell. The target voltage scales with hard x-ray emission, which in turn has been previously shown to correlate with TPD-generated hot-electrons.

implosions is the TPD-instability. This was determined by observing a correlation between the hard x-ray signal from bremsstrahlung radiation (photon energies >40 keV, produced by hot-electrons stopping on the shell) and the $3\omega/2$ signal, a signature of the TPD-instability. In this work, we observe a correlation between the hard x-ray signal and the target voltage (Fig. 5), confirming that the TPD-generated electrons accelerate the ions presented in this work.

In summary, the first measurements of the total energy carried by fast ablator-ions on OMEGA have been conducted. It has been shown that the total energy carried by fast ablator-ions is $\lesssim$1% of the incident laser energy. These measurements have been used to infer a non-linear, voltage-dependent target capacitance associated with the sheath fields surrounding the target. The peak target voltage scales linearly with laser intensity for a range of targets, with a dependence on shell thickness and to some extent, shell material. It was observed that the target voltage is correlated with the hard x-ray signal, previously shown to scale with TPD-generated hot-electrons, confirming the mechanism behind charging of these targets at OMEGA. Future studies will use these ion measurements to build a model for the target potential time-dependence. Such a model can be used with hot-electron measurements to estimate preheat in direct-drive OMEGA targets.

The authors express their gratitude to Ernie Doeg and Robert Frankel (MIT) for CR-39 processing and Dino Mastrosimone (LLE) for engineering support. This work was supported in part by NLUF/DOE (Grant No. DE-FG03-03SF22691), LLE (No. 412160-001G), LLNL (No. B504974), and GA under DOE (DE-AC52-06NA27279).

[1]D. G. Hicks, C. K. Li, F. H. Séguin, J. D. Schnittman, A. K. Ram, J. A. Frenje, R. D. Petrasso, J. M. Soures, D. D. Meyerhofer, S. Roberts, C. Sorce, C. Stockl, T. C. Sangster, and T. W. Phillips, "Observations of fast protons above 1 MeV produced in direct-drive laser-fusion experiments," Phys. Plasmas **8**(2), 606–610 (2001).
[2]A. B. Zylstra, C. K. Li, F. H. Séguin, M. J. Rosenberg, H. G. Rinderknecht, N. Sinenian, J. A. Frenje, R. D. Petrasso, N. Izumi, P. A. Amendt, O. L. Landen, and J. A. Koch, "Measurements of hohlraum-produced fast ions," Phys. Plasmas **19**(4), 042707 (2012).
[3]T. R. Boehly, D. L. Brown, R. S. Craxton, R. L. Keck, J. P. Knauer, J. H. Kelly, T. J. Kessler, S. A. Kumpan, S. J. Loucks, S. A. Letzring, F. J. Marshall, R. L. McCrory, S. F. B. Morse, W. Seka, J. M. Soures, and C. P. Verdon, "Initial performance results of the OMEGA laser system," Opt. Commun. **133**(1–6), 495–506 (1997).
[4]T. H. Tan, G. H. McCall, and A. H. Williams, "Determination of laser intensity and hot-electron temperature from fastest ion velocity measurement on laser-produced plasma," Phys. Fluids **27**(1), 296–301 (1984), and references therein.
[5]F. N. Beg, A. R. Bell, A. E. Dangor, C. N. Danson, A. P. Fews, M. E. Glinsky, B. A. Hammel, P. Lee, P. A. Norreys, and M. Tatarakis, "A study of picosecond laser–solid interactions up to 10^{19} W-cm^{-2}," Phys. Plasmas **4**(2), 447–457 (1997).
[6]D. G. Hicks, C. K. Li, F. H. Séguin, A. K. Ram, J. A. Frenje, R. D. Petrasso, J. M. Soures, V. Yu Glebov, D. D. Meyerhofer, S. Roberts, C. Sorce, C. Stoeckl, T. C. Sangster, and T. W. Phillips, "Charged-particle acceleration and energy loss in laser-produced plasmas," Phys. Plasmas **7**(12), 5106–5117 (2000).
[7]M. J.-E. Manuel, N. Sinenian, F. H. Séguin, C. K. Li, J. A. Frenje, H. G. Rinderknecht, D. T. Casey, A. B. Zylstra, R. D. Petrasso, and F. N. Beg, "Mapping return currents in laser-generated z-pinch plasmas using proton deflectometry," Appl. Phys. Lett. **100**(20), 203505 (2012).
[8]J. S. Pearlman and G. H. Dahlbacka, "Charge separation and target voltages in laser-produced plasmas," Appl. Phys. Lett. **31**(7), 414–417 (1977).
[9]R. F. Benjamin, G. H. McCall, and A. W. Ehler, "Measurement of return current in a laser-produced plasma," Phys. Rev. Lett. **42**, 890–893 (1979).
[10]W. L. Kruer, *The Physics Of Laser Plasma Interactions* (Westview, 2003).
[11]D. H. Froula, B. Yaakobi, S. X. Hu, P-Y. Chang, R. S. Craxton, D. H. Edgell, R. Follett, D. T. Michel, J. F. Myatt, W. Seka, R. W. Short, A. Solodov, and C. Stoeckl, "Saturation of the two-plasmon decay instability in long-scale-length plasmas relevant to direct-drive inertial confinement fusion," Phys. Rev. Lett. **108**, 165003 (2012), and references therein.
[12]V. N. Goncharov, T. C. Sangster, P. B. Radha, R. Betti, T. R. Boehly, T. J. B. Collins, R. S. Craxton, J. A. Delettrez, R. Epstein, V. Yu. Glebov, S. X. Hu, I. V. Igumenshchev, J. P. Knauer, S. J. Loucks, J. A. Marozas, F. J. Marshall, R. L. McCrory, P. W. McKenty, D. D. Meyerhofer, S. P. Regan, W. Seka, S. Skupsky, V. A. Smalyuk, J. M. Soures, C. Stoeckl, D. Shvarts, J. A. Frenje, R. D. Petrasso, C. K. Li, F. Seguin, W. Manheimer, and D. G. Colombant, "Performance of direct-drive cryogenic targets on OMEGA," Phys. Plasmas **15**(5), 056310 (2008).
[13]N. Sinenian, "An empirical target discharging model for direct-drive implosions on OMEGA" (unpublished).
[14]F. H. Séguin, J. A. Frenje, C. K. Li, D. G. Hicks, S. Kurebayashi, J. R. Rygg, B. E. Schwartz, R. D. Petrasso, S. Roberts, J. M. Soures, D. D. Meyerhofer, T. C. Sangster, J. P. Knauer, C. Sorce, V. Yu Glebov, C. Stoeckl, T. W. Phillips, R. J. Leeper, K. Fletcher, and S. Padalino, "Spectrometry of charged particles from inertial-confinement-fusion plasmas," Rev. Sci. Instrum. **74**(2), 975–995 (2003).
[15]J. A. Cobble, K. A. Flippo, D. T. Offermann, F. E. Lopez, J. A. Oertel, D. Mastrosimone, S. A. Letzring, and N. Sinenian, "High-resolution thomson parabola for ion analysis," Rev. Sci. Instrum. **82**(11), 113504 (2011).
[16]N. Sinenian, M. J. Rosenberg, M. Manuel, S. C. McDuffee, D. T. Casey, A. B. Zylstra, H. G. Rinderknecht, M. G. Johnson, F. H. Séguin, J. A. Frenje, C. K. Li, and R. D. Petrasso, "The response of CR-39 nuclear track detector to 1-9 MeV protons," Rev. Sci. Instrum. **82**(10), 103303 (2011).
[17]A. Simon, R. W. Short, E. A. Williams, and T. Dewandre, "On the inhomogeneous two-plasmon instability," Phys. Fluids **26**(10), 3107–3118 (1983).
[18]Y. Lin, T. J. Kessler, and G. N. Lawrence, "Distributed phase plates for super-gaussian focal-plane irradiance profiles," Opt. Lett. **20**(7), 764–766 (1995).
[19]T. R. Boehly, V. A. Smalyuk, D. D. Meyerhofer, J. P. Knauer, D. K. Bradley, R. S. Craxton, M. J. Guardalben, S. Skupsky, and T. J. Kessler, "Reduction of laser imprinting using polarization smoothing on a solid-state fusion laser," J. Appl. Phys. **85**(7), 3444–3447 (1999).
[20]S. P. Regan, J. A. Marozas, J. H. Kelly, T. R. Boehly, W. R. Donaldson, P. A. Jaanimagi, R. L. Keck, T. J. Kessler, D. D. Meyerhofer, W. Seka, S. Skupsky, and V. A. Smalyuk, "Experimental investigation of smoothing by spectral dispersion," J. Opt. Soc. Am. B **17**(9), 1483–1489 (2000).
[21]B. Yaakobi, P.-Y. Chang, A. Solodov, C. Stoeckl, D. H. Edgell, R. S. Craxton, S. X. Hu, J. F. Myatt, F. J. Marshall, W. Seka, and D. H. Froula, "Fast-electron generation in long-scale-length plasmas," Phys. Plasmas **19**(1), 012704 (2012).
[22]P. Mora, Phys. Rev. Lett. **90**, 185002 (2003).
[23]C. Stoeckl, V. Yu. Glebov, D. D. Meyerhofer, W. Seka, B. Yaakobi, R. P. J. Town, and J. D. Zuegel, "Hard x-ray detectors for OMEGA and NIF," Rev. Sci. Instrum. **72**(1), 1197–1200 (2001).
[24]W. Seka, D. H. Edgell, J. P. Knauer, J. F. Myatt, A. V. Maximov, R. W. Short, T. C. Sangster, C. Stoeckl, R. E. Bahr, R. S. Craxton, J. A. Delettrez, V. N. Goncharov, I. V. Igumenshchev, and D. Shvarts, "Time-resolved absorption in cryogenic and room-temperature direct-drive implosions," Phys. Plasmas **15**(5), 056312 (2008).